A Molecular Z-Scheme Artificial Photosynthetic System Under the Bias-Free Condition for CO2 Reduction Coupled with Two-electron Water Oxidation: Photocatalytic Production of CO/HCOOH and H2O2

Kuttassery, Fazalurahman

Ohsaki, Yutaka

Thomas, Arun

Kamata, Ryutaro

他

出版情報：Angewandte Chemie International Edition. 62 (40), 2023-08-24. Wiley
バージョン：

How to cite: *Angew. Chem. Int. Ed.* **2023**, *62*, e202308956
doi.org/10.1002/anie.202308956

Artificial Photosynthesis | Hot Paper

A Molecular Z-Scheme Artificial Photosynthetic System Under the Bias-Free Condition for CO_2 Reduction Coupled with Two-electron Water Oxidation: Photocatalytic Production of CO/HCOOH and H_2O_2

Fazalurahman Kuttassery, Yutaka Ohsaki, Arun Thomas, Ryutaro Kamata, Yosuke Ebato, Hiromu Kumagai, Ryosuke Nakazato, Abin Sebastian, Siby Mathew, Hiroshi Tachibana, Osamu Ishitani,* and Haruo Inoue**

Abstract: Bio-inspired molecular-engineered systems have been extensively investigated for the half-reactions of H_2O oxidation or CO_2 reduction with sacrificial electron donors/acceptors. However, there has yet to be reported a device for dye-sensitized molecular photoanodes coupled with molecular photocathodes in an aqueous solution without the use of sacrificial reagents. Herein, we will report the integration of Sn^{IV}- or Al^{III}-tetrapyridylporphyrin (SnTPyP or AlTPyP) decorated tin oxide particles (SnTPyP/SnO_2 or AlTPyP/SnO_2) photoanode with the dye-sensitized molecular photocathode on nickel oxide particles containing $[Ru(diimine)_3]^{2+}$ as the light-harvesting unit and $[Ru(diimine)(CO)_2Cl_2]$ as the catalyst unit covalently connected and fixed within poly-pyrrole layer (RuCAT-RuC_2-*PolyPyr*-PRu/NiO). The simultaneous irradiation of the two photoelectrodes with visible light resulted in H_2O_2 on the anode and CO, HCOOH, and H_2 on the cathode with high Faradaic efficiencies in purely aqueous conditions without any applied bias is the first example of artificial photosynthesis with only two-electron redox reactions.

Introduction

The unanticipated consequences of rising CO_2 emissions and climate change are looming on a global scale.[1] Among the various approaches to carbon capture and utilization, direct photochemical fixation of CO_2 with water as an electron donor is one of the most promising global challenges.[2] Since Lehn et al. discovered the photochemical reduction of CO_2 into CO catalyzed by Re^I complexes as one of the critical milestones in modern artificial photosynthesis,[3] much effort has been devoted to developing a benchmark reaction and improving reactivity, and intensive studies on the reaction mechanism.[4] Following the Re-complexes, various other metal-complexes, such as Ru^{II}-,[5] Ir^{III}-[6] Cu^I-,[7] Co^{II}-,[8] Ni^{II}-,[9] Mn^I-,[10] and Fe^{II}-complexes,[11] have been reported to electrochemically/photochemically catalyze CO_2 reduction. Because of their superior properties, such as photo- and thermal stability, high reduction ability, and extremely low absorption in the visible region without interfering with light harvesting by a redox photosensitizer, *trans*(Cl)-[Ru(diimine)$(CO)_2Cl_2$]-type catalysts have been widely used in various photocatalytic systems for CO_2 reduction.[5b,12] Many photocatalytic CO_2 reduction systems, consisting of metal-complex catalysts and redox photosensitizers that initiate a

[*] Dr. F. Kuttassery
Department of Chemistry, University of Calicut
Malappuram, Kerala, 673635 (India)
E-mail: kfazalurahman@uoc.ac.in

Y. Ohsaki, R. Nakazato, Dr. A. Sebastian, Dr. S. Mathew, Prof. H. Tachibana, Prof. H. Inoue
Department of Applied Chemistry for Environment, Graduate School of Urban Environmental Sciences, Tokyo Metropolitan University
1-1 Minami Osawa, Hachioji, Tokyo, 192-0397 (Japan)
E-mail: inoue-haruo@tmu.ac.jp

Dr. A. Thomas
Department of Chemistry, St. Stephen's College
Uzhavoor, Kerala, 686634 (India)

R. Kamata, Y. Ebato, Prof. O. Ishitani
Department of Chemistry, Tokyo Institute of Technology
2-12-1-NE-1 O-okayama, Meguro, Tokyo, 152-8550 (Japan)
E-mail: ishitani@chem.titech.ac.jp

Dr. H. Kumagai
Research Center for Advanced Science and Technology, The University of Tokyo
4-6-1 Komaba, Meguro, Tokyo, 153-8904 (Japan)

Prof. O. Ishitani
Department of Chemistry, Graduate School of Advanced Science and Engineering, Hiroshima University
1-3-1 Kagamiyama, Higashi-Hiroshima, Hiroshima, 739-8526 (Japan)

single photochemical electron transfer from the reductant to the catalyst, exhibit high photocatalytic properties such as high quantum yield, durability, and product selectivity.[2b,5b,13] Due to the low oxidation power of the redox photosensitizers in the excited state, these systems require sacrificial electron donors such as amines and ascorbic acid. The incorporation of water molecules into these systems is another challenging issue owing to the limitations of using sacrificial electron donors in molecular catalyst systems for CO_2 reduction. Pioneering reports on hybrid systems combining molecular photocatalysts (MCs) for CO_2 reduction with semiconductors for water oxidation,[2b,14] as well as fully semiconductor systems for both terminal ends,[2c,15] have appeared. High energy conversion efficiencies have also been reported for electrochemical molecular catalyst systems coupled with photovoltaic devices.[16] These reports on photochemical CO_2 fixation with water as an electron donor, however, have focused on the evolution of dioxygen as a water oxidation reaction on metal oxides. Conversely, photochemical water oxidation to generate O_2 by MCs has long been hampered by the bottleneck, "Photon-flux-density problem of sunlight,"[17] caused by rarefied solar radiation. To reach a higher oxidation state (+4), water oxidation requires four-electron oxidation via sequential four-photon processes. The rarefied photon flux density of sunlight forces MCs to wait for the next photon's arrival in by far the longer timescale up to the second order than the inherent one of molecules within ≈μs, which inevitably leads to unexpected transformation/decomposition of MCs during the long waiting period to suffer many collisional processes with impurities and solvent molecules and to lose water oxidation activity. However, another mode of water oxidation, such as a two-electron process forming H_2O_2 induced by one-photon excitation of MCs, has been developed,[17c] which does not require waiting for the next photon to avoid the "Photon-flux-density problem."[17] Hydrogen peroxide is one of the most useful chemicals and would be far superior to O_2 as a water oxidation product due to higher energy storage (1.77 V for H_2/H_2O_2 vs. 1.23 V for $2H_2/O_2$) and easier separation of the products (H_2, CO(gas)/H_2O_2(liquid)) than H_2, CO(gas)/O_2(gas).[17c] Coupling CO_2 fixation at the reduction terminal with H_2O_2 formation at the oxidation terminal is one of the most promising targets, leading to more practical and useful artificial photosynthesis.[17c,18] We attempted to construct a Z-scheme-type artificial photosynthetic system consisting of a photoanode with a molecular photocatalyst for two-electron water oxidation into H_2O_2 and a photocathode with a molecular photocatalyst for CO_2 reductive fixation. A novel molecular catalyst photocathode for CO_2 reduction, a Ru-based molecular photosensitizer, and catalyst units immobilized on NiO particles using a polypyrrole layer, which exhibits stable reactivity even after extended visible-light irradiation, have recently been developed.[19] Using this molecular catalyst photocathode (MC-photocathode), we have fabricated a new "Molecular catalyst photoanode (MC-photoanode)" capable of driving two-electron water oxidation to form H_2O_2 for the construction of a Z-scheme type artificial photosynthetic system. Crucial points in designing the MC-photoanode would be 1) tuning the redox character with the MC-photocathode (Ru-based photosensitizer + catalyst/NiO) to drive the Z-scheme system using only visible light as energy source, i.e., under the "Bias free" condition, 2) minimizing the unfavorable desorption of the molecular catalyst from the photoanode substrate during the reaction, 3) maximizing the oxidation ability of forming H_2O_2 from water, 4) exhibiting reactions of CO_2 fixation and H_2O_2 formation under nearly neutral conditions (pH 5–9), and 5) easy preparation with most available elements. Based on these design guidelines, we chose water-insoluble $[Sn^{IV}TPyP(O^-)_2]^{2-}$ (*trans*-dioxo-coordinated 5, 10, 15, 20-tetra(4-pyridyl)porphyrinatetin (IV): SnTPyP) with doubly deprotonated axial ligands ($-O^-$) under neutral conditions as a novel visible-light-absorbing molecular catalyst for two-electron water oxidation. Another water-insoluble molecular catalyst is $[Al^{III}TPyP(OH)_2]^-$ (*trans*-dihydroxy-coordinated 5, 10, 15, 20-tetra(4-pyridyl) porphyrinate aluminum (III): AlTPyP) with hydroxy axial ligands (−OH) was also used as a reference molecular catalyst. These metalloporphyrins have sufficient hole potentials to drive the two-electron oxidation of water to H_2O_2 following one-electron oxidation of the porphyrin ring via photochemical or electrochemical initiation.[20]

An *n*-type semiconductor (SnO_2 nanoparticles) was then selected as the substrate of the MC photoanode to fabricate Sn^{IV}- or Al^{III}-tetrapyridylporphyrin (SnTPyP or AlTPyP) decorated tin oxide particles (SnTPyP/SnO_2 or AlTPyP/SnO_2) through covalent bond formation between the axial ligands of SnTPyP or AlTPyP and the surface OH groups on SnO_2, which allowed exergonic electron flow to the NiO substrate of the MC-photocathode under bias-free conditions.

In this study, we report the first successful artificial photosynthesis construction that can drive CO_2 reduction on (Ru-complex photosensitizer + catalyst)/NiO as a dye-sensitized MC photocathode and H_2O_2 formation from water on SnTPyP/SnO_2 or AlTPyP/SnO_2 as MC photoanodes using only visible light as an energy source without any external bias. In terms of solar energy conversion, this reaction produces H_2O_2 from water (equations. 2 and 4) and can accumulate significantly more energy than conventional systems that produce O_2 (equations. 1 and 3).

	ΔG^0 / kJ. mol^{-1}	
$H_2O + CO_2 \longrightarrow HCOOH + ½\ O_2$	259	(1)
$2H_2O + CO_2 \longrightarrow HCOOH + H_2O_2$	362	(2)
$CO_2 \longrightarrow CO + ½\ O_2$	257	(3)
$H_2O + CO_2 \longrightarrow CO + H_2O_2$	360	(4)

Results and Discussion

In designing photoanodes for water oxidation, we developed two types of MC photoanodes, that is, SnTPyP or AlTPyP (MTPyP, Figure 1), both of which can photocatalyze the

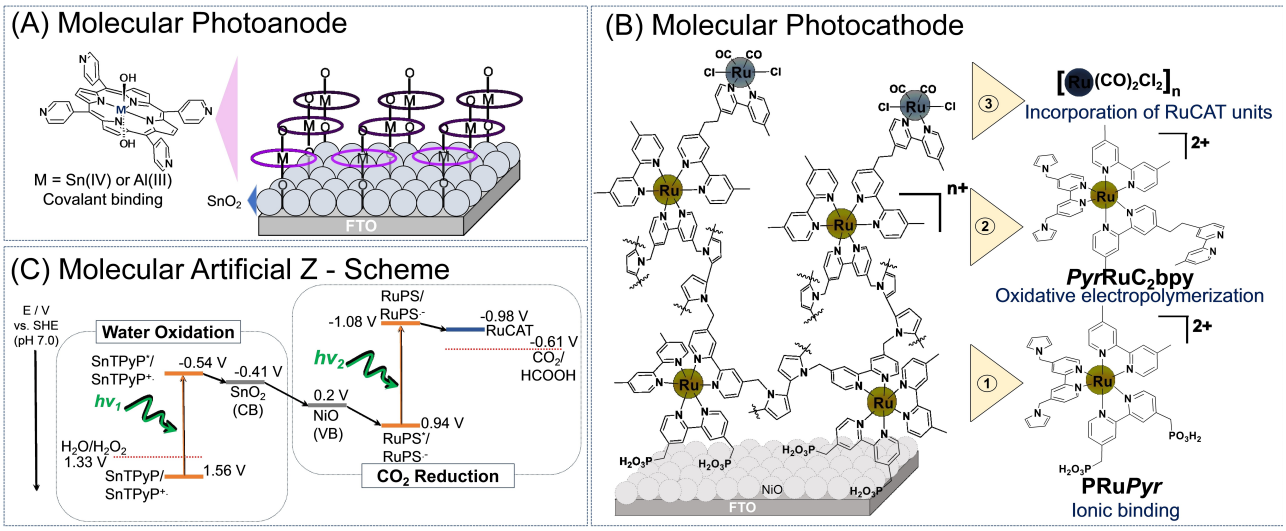

Figure 1. (A) Structure of the MTPyP molecular catalyst and their covalently immobilized photoanode: (B) Molecular structure of Ru based molecular photosensitizer and catalyst units immobilized on NiO particles using a poly pyrrole layer; (C) Molecular artificial Z- scheme for the reduction of CO_2 by using water as the reductant.

two-electron oxidation of water to form H_2O_2, on a SnO_2 *n*-type semiconductor electrode (SnTPyP/SnO_2 or AlTPyP/SnO_2), which was fabricated through covalent adsorption between the axial ligands of MTPyP and the surface OH group of SnO_2 (Figure 1A, see experimental (SI)). Cyclic voltammetry of SnTPyP or AlTPyP in CH_3CN/H_2O (8/2, *v*/*v*) with 0.1 M $TBAPF_6$ as the supporting electrolyte at neutral pH revealed catalytic oxidation waves at 1.56 V vs SHE for SnTPyP[20c] and 1.26 V vs SHE for AlTPyP.[20b] Because the excited energy of these metalloporphyrins is ≈2.1 eV[21] in their singlet excited states, visible light irradiation of the photoanode (SnTPyP or AlTPyP adsorbed on the surface of SnO_2 ($E_{conduction\ band} \approx -0.41$ V vs SHE at pH 7)[22] would surely induce an electron injection from the excited MTPyP into the conduction band of SnO_2 ($\Delta G = \approx -0.13$ eV for SnTPyP and $\Delta G = \approx -0.43$ eV for AlTPyP) (Figure 1C). Because the electrochemically formed one-electron oxidized species of SnTPyP and AlTPyP drive water oxidation into H_2O_2,[23] visible light irradiation of the MC photoanode in water was investigated to see if an anodic photocurrent and the formation of H_2O_2 as the water oxidation product was induced. In a three-component cell with a SnTPyP/SnO_2 or AlTPyP/SnO_2 photoelectrode as the working electrode, Ag/AgCl (saturated KCl) as the reference electrode, and a Pt coil as the counter electrode, photoelectrochemical experiments for water oxidation on the MC photoanode were performed. The linear sweep voltammograms (LSV) for SnTPyP/SnO_2 and AlTPyP/SnO_2 photoelectrodes revealed distinct photo-responsive anodic currents: Anodic currents began to appear at ≈−0.05 V vs Ag/AgCl in both cases and became stable at the more positive potential > ≈ +0.1 V vs Ag/AgCl for SnTPyP/SnO_2 (≈40 μA: Figure 2A) and AlTPyP (≈15 μA: Figure 2 b), respectively, following visible light irradiation (λ = 420 nm, 0.8 mW cm^{-2}).

In designing artificial photosynthesis consisting of molecular photocatalysts that perform CO_2 reduction by utilizing electrons from water, we attempted to combine the MC photoanodes described above with a dye-sensitized molecular photocathode (MC photocathode) consisting of [Ru(diimine)$_3$]$^{2+}$-type complexes as light-harvesting units and a Ru (diimine)$(CO)_2Cl_2$ type complex as a catalyst unit, both of which were covalently connected and fixed in and on a polypyrrole layer on the NiO electrode (RuCAT-RuC_2-*PolyPyr*-PRu/NiO) (Figure 1B).[19] The MC-photocathode demonstrated its photocathodic response (λ > 460 nm, 28.2 mW cm^{-2}) starting from a relatively positive potential (E = +0.3 V vs Ag/AgCl, red lines in Figure 2) in CO_2-bubbled aqueous solution containing 50 mM $NaHCO_3$ as the electrolyte (pH = 6.6).[19] Since the conduction band of SnO_2 (≈−0.41 V vs SHE at pH 7)[22a] is situated above the valence band of NiO (+0.2 V vs SHE at pH 7),[24] an exergonic electron flow from the conduction band of SnO_2 (injected electrons from the excited SnTPyP or AlTPyP) to the valence band of NiO (injected holes from the excited Ru photosensitizer units) would be surely expected when the MC-photoanodes are coupled with the MC-photocathode (Figure 1C). Both the anodic and cathodic photocurrents were observed to well overlap at the potential region, −0.05–+0.2 V vs Ag/AgCl, indicating that full-cell device consisting of photoanodes and photocathodes would be promisingly working for electron transport from H_2O to CO_2 without any external bias potential applied (Figure 2).

The formation of H_2O_2 as a water-oxidation product on the MC photoanode was investigated prior to the construction of the full-cell device (Figure S1). A colorimetric method with Ti^{IV}-tetrapyridylporphyrin (TiTPyP) as the sensor was used for the SnTPyP/SnO_2 photoanode (Figure S2).[23a,25] H_2O_2 was detected in the half-cell reaction at +0.1 V vs Ag/AgCl in water (([$NaHCO_3$] = 50 mM) for 2-h irradiation (λ = 420 nm, 0.8 mW cm^{-2}) in the amount of

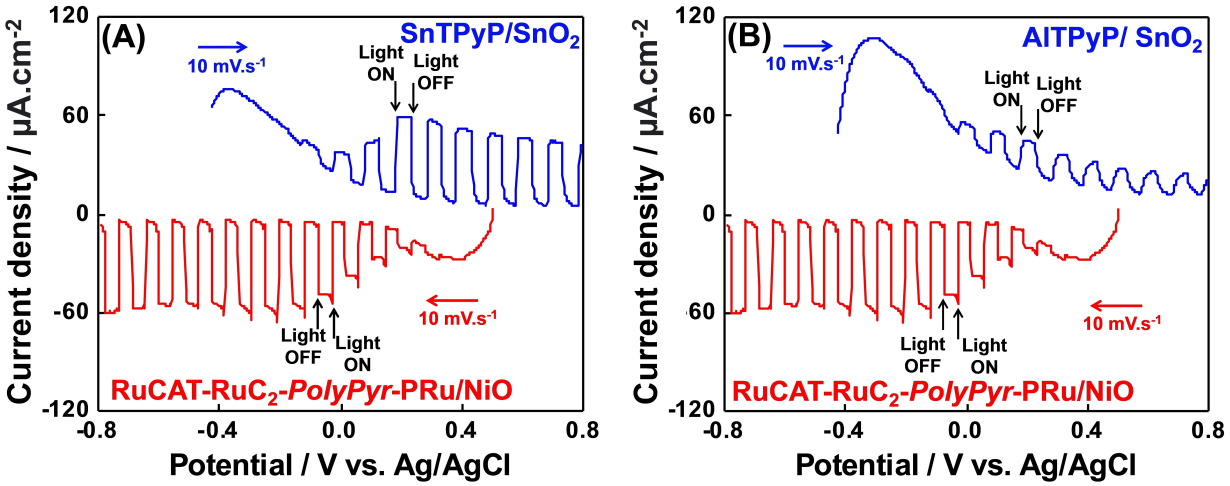

Figure 2. *I–V* curves of (A) SnTPyP/SnO_2 under irradiation of light ($\lambda = 420$ nm, 1.3 mW cm^{-2}) photoanode and RuCAT-RuC_2-*PolyPyr*-PRu/NiO photocathode under irradiation of light ($\lambda = 460$–650 nm, 28.2 mW cm^{-2}) (B) AlTPyP/SnO_2 under irradiation of light ($\lambda = 420$ nm, 1.3 mW cm^{-2}) photoanode and RuCAT-RuC_2-*PolyPyr*-PRu/NiO photocathode ($\lambda = 460$–650 nm, 28.2 mW cm^{-2}) in CO_2 bubbled aqueous $NaHCO_3$ solution (pH 6.6, reference electrode: Ag/AgCl (Saturated KCl), counter electrode: Pt wire).

32 nmol (Turnover Number (TON) = 4.6). When the gas phase in the half cell reaction system was checked using a gas chromatograph equipped with a thermal conductivity detector and nitrogen as the carrier gas, O_2 was not detected after 2 h of light irradiation. These findings suggest that H_2O_2 was the only oxidation product of water on the SnTPyP/SnO_2 photoanode in the photoelectrochemical system, as observed in the AlTCPP/TiO_2 photochemical system.[26] A similar photocatalytic reaction using AlTPyP/SnO_2 as the MC-photoanode instead of SnTPyP/SnO_2 showed a selective formation of H_2O_2 in the amount of 15 nmol (TON = 3.1) in the half-cell experiment for 2 h (Figure S1B, $\lambda = 420$ nm, 0.8 mW cm^{-2}), though the reactivity was less than SnTPyP/SnO_2 as observed in the LSV (Figure 2). The lower reactivity of AlTPyP/SnO_2 was explained by the following theoretical DFT calculations. The one-electron oxidized form of $[SnTPyP(O^-)_2]^{2-}$ with deprotonated axial ligands ($-O^-$) in a doublet electronic spin state has its electron spin exclusively localized on the axial oxygen atom as oxyl radical ($-O^\bullet$) that serves as a key intermediate in H_2O_2 formation, whereas the electron spin of the one-electron oxidized form of $[AlTPyP(OH)_2]^-$ having protonated axial ligands ($-OH$) mostly delocalized over the porphyrin ring that would be less reactive against H_2O_2 formation (Figure S3). The higher oxidation potential of SnTPyP (1.56 V vs SHE) compared to AlTPyP (1.26 V vs SHE) also explains the differences in reactivities for two-electron oxidation of water into H_2O_2. Both factors would simultaneously control the reactivity.

To confirm the origin of the oxygen atoms in the produced H_2O_2, SnTPyP/SnO_2 was subjected to isotope labeling experiments with $H_2{}^{18}O$ ($H_2{}^{18}O/H_2{}^{16}O = 1/9$, v/v). GC-MS is used to estimate the uptake of ^{18}O in the forms of ^{16}O–^{18}O and ^{18}O–^{18}O in O_2 via an enzymatic reaction with catalase to convert H_2O_2 into O_2. As shown in Figure 3, treatment of the reaction mixture with the enzyme catalase resulted in an increase in ^{16}O–^{18}O and ^{18}O–^{18}O, but a

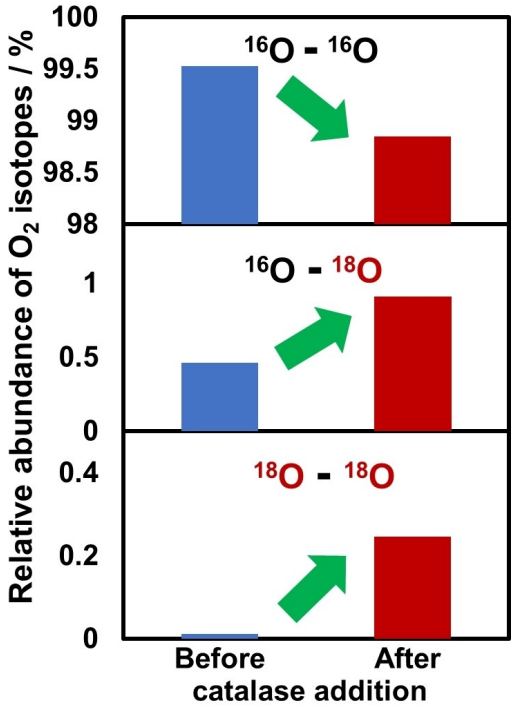

Figure 3. Isotope experiment using 10% O-18 enriched water in the electrolyte solution to demonstrate the source of oxygen in H_2O_2 as the water. before and after adding the catalase enzyme to the phosphate buffer, O_2 isotope profiling was performed.

decrease in ^{16}O–^{16}O (Figure 3), indicating that the oxygen atom of H_2O_2 originated from H_2O. These results confirm that irradiating the MC photoanode (SnTPyP/SnO_2) to visible-light induces selective two-electron oxidation of water to produce H_2O_2. The results of isotope labelled experiments clearly suggest the produced H_2O_2 originates from the water molecules. The electrolyte species bicarbonate (HCO_3^-) ions might provide a promotive path for the

formation of H_2O_2 through peroxo-carbonate (HCO_4^-) intermediate which prevents the further oxidation of peroxides into molecular oxygen in the catalytic cycle.[25b,27]

Based on the results of the half-cell reactions, we can anticipate that simultaneous visible-light irradiation of both electrodes induces electron flow from SnTPyP or AlTPyP in the MC photoanode to the Ru catalyst in the MC photoanode without the use of an external bias (Figure 1C). A complete cell was built, with a SnTPyP/SnO_2 MC-photoanode and a RuCAT-RuC_2-*PolyPyr*-PRu/NiO MC-photocathode connected and set up in each compartment separated by a Nafion® membrane. Under the bubbling of CO_2 (pH 6.6), the two compartments were filled with an aqueous solution containing 50 mM $NaHCO_3$ as the electrolyte. The good overlap of the LSV curves between the SnTPyP/SnO_2 MC photoanode and the RuCAT-RuC_2-*PolyPyr*-PRu/NiO MC photocathode (Figure 2) indicates that these two pairs of photoelectrodes can be used as a fully molecular artificial Z-scheme system with no external bias. First, the requirement for simultaneous excitation of both the MC photoanode and photocathode was tested by maintaining one of the photoelectrodes in the dark. When one electrode was irradiated with visible light, whereas the other was kept in the dark, only a small number of electrons flowed between the photoelectrodes, as shown in Figure 4A. Under simultaneous excitation with monochromatic light at 420 nm for the MC photoanode (2.7 mW cm^{-2}) and 480 nm for the MC-photocathode (3.5 mW cm^{-2}), a rather stable photocurrent of 7 μA was observed.

The photoelectrochemical CO_2 reduction was then tested in the zero-resistance ammeter mode, when the wavelengths of light irradiation were chosen for the MC-photoanode (SnTPyP/SnO_2) as $\lambda = 420$ nm (1.32 mW cm^{-2}) and for the MC-photocathode (RuCAT-RuC_2-*PolyPyr*-PRu/NiO) as 460 nm $< \lambda <$ 650 nm (27.8 mW cm^{-2}) to maintain the catalytic activities of photoelectrodes. The MC-photocathode (RuCAT-RuC_2-*PolyPyr*-PRu/NiO) remained unchanged without desorption of the catalyst, while the MC-photoanode (SnTPyP/SnO_2) suffered a slight desorption of SnTPyP without decomposition (Figure S4). The degree of desorption of SnTPyP was much smaller than that in the half-cell reaction where the pH of the reaction mixture

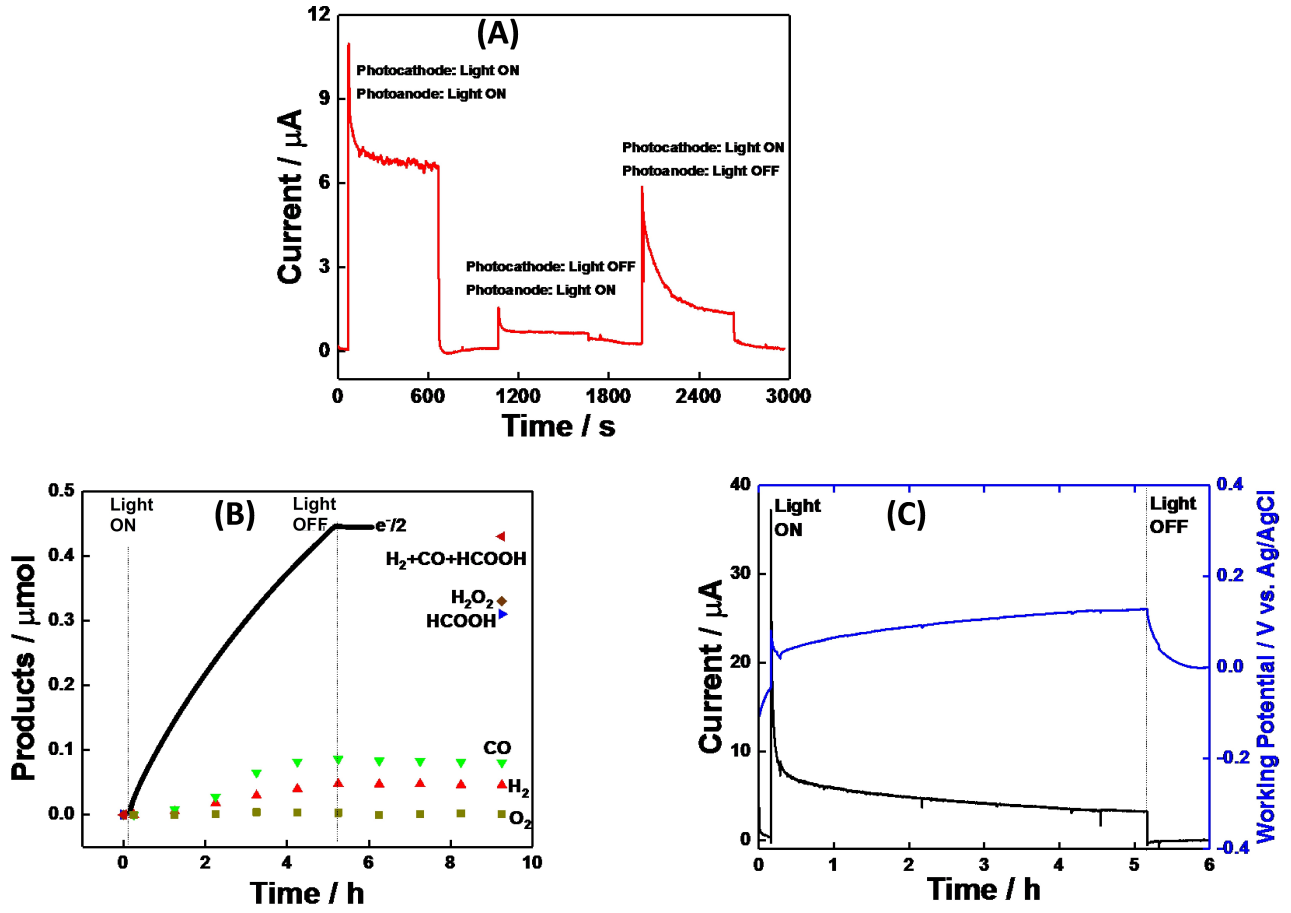

Figure 4. (A) Photo-response on the *I-t* plot of full-cell constructed using SnTPyP/SnO_2 MC-photoanode and RuCAT-RuC_2-*PolyPyr*-PRu/NiO MC-photocathode without any bias applied. The MC-photoanode and MC-photocathode in pure water containing $NaHCO_3$ under the CO_2 bubbling (pH 6.6) were irradiated with $\lambda = 420$ nm (2.7 mW cm^{-2}) and $\lambda = 480$ nm (3.5 mW cm^{-2}), respectively, (B) amounts of the reaction products, O_2, H_2O_2, from the anode compartment and CO, HCOOH, and H_2, from the cathode compartment respectively: the MC-photocathode was irradiated with the light of 460 nm $< \lambda <$ 650 nm (27.8 mW cm^{-2}) and the MC-photoanode was done with $\lambda = 420$ nm (1.32 mW cm^{-2}), (C) photocurrent (black) and working potential (blue) for 5 h's light irradiation.

might decrease to cause the desorption because the pH should be maintained in the full-cell reaction where OH^- is consumed on the MC-photoanode and H^+ is consumed on the MC-photocathode. For more than 5 h, a relatively stable photocurrent was observed (Figure 4C). After 5 h of light irradiation, the photocathode produced primarily HCOOH (310 nmol), with minor amounts of CO (86 nmol) and H_2 (48 nmol) also detected. In the photoanode compartment, H_2O_2 (330 nmol) was only detected in the solution, while O_2 was not detected in the gas phase even after 5 h of irradiation (Figure 4B). On the photocathodic and photoanodic sides, the Faradaic efficiencies of the reduction and oxidation reactions were calculated to be 95.4 and 72.7 %, respectively. We demonstrate that the firstly reported fully molecular two-electron approach for simultaneous production of H_2O_2 and CO/HCOOH has comparable Faradaic efficiencies and energy conversion efficiencies with the reported Z-scheme systems integrated four-electron oxidation of water by using semiconductor based photoanodes (Table S1). The turnover number (TONs) was 17.8 for the reduction products and 47.3 for H_2O_2 based on the catalyst units used on each photoelectrode (Table 1).

These findings indicate that the molecular units on both photoelectrodes are catalytically cycled during the photo-induced reactions of selective two-electron oxidation of water to H_2O_2 and CO_2 reduction in an aqueous solution without any applied bias. The efficiency of photo- to chemical-energy conversion for the full cell reaction for CO_2 reduction coupled with H_2O_2 generation from water was discovered to be $\approx 1.2\times10^{-2}$%.

Conclusion

The selective two-electron oxidation of water to H_2O_2 was demonstrated by one-photon excitation of SnTPyP or AlTPyP molecules adsorbed on SnO_2 as the MC photoanode. These MC photoanodes were successfully combined with an MC photocathode composed of polypyrrole layers immobilizing a supramolecular photocatalyst (RuCAT) fixed on NiO to fabricate the first example of molecular Z-scheme-type full-cell devices capable of inducing both photocatalytic reactions of two-electron water oxidation into H_2O_2 and CO_2 reduction to HCOOH/CO upon visible light irradiation. The photoelectrochemical full-cell combination of SnTPyP/SnO_2 and RuCAT-RuC_2-*PolyPyr*-PRu/NiO, in particular, exhibits good photocatalytic activity.

Supporting Information

Experimental details and additional data for supporting the findings in the manuscript have included in the Supporting Information.

Acknowledgements

This work was supported by JST CREST grant number JPMJCR13L1 in "Molecular Technology," JST Strategic International Collaborative Research Program (PhotoCAT), and JSPS KAKENHI Grant numbers JP20H00396, JP17H06439 and JP17H06440 in Scientific Research on Innovative Areas "Innovations for LightEnergy Conversion (I4LEC)". F.K. thanks Department of Science and Technology (DST), Government of India for DST-INSPIRE Faculty Grant (IFA19-CH320) and DST-SERB Start-up Grant (SRG/2022/002097).

Conflict of Interest

The authors declare no conflict of interest.

Data Availability Statement

The data that support the findings of this study are available in the supplementary material of this article.

Keywords: CO_2 Reduction · Photocatalytic Reactions · Photoelectrochemical Cell · Selective Formation of H_2O_2 · Water Oxidation

Table 1: Summary of photoelectrochemical CO_2 reduction by RuCAT-RuC_2-*PolyPyr*-PRu/NiO photocathode in the full cell system using MTPyP/SnO_2 photoanode in CO_2 purged 50 mM $NaHCO_3$ solution (pH 6.6) (Photocathode: λ_{ex} = 460–650 nm, 27.8 mW cm^{-2}, photoanode: λ_{ex} = 420 nm, 1.32 mW cm^{-2}).

	Oxidation at MC-photoanode			Reduction at MC-photocathode				
Photoanode	H_2O_2 /nmol (TON)[a]	O_2 /nmol	F.Y.[b] (%)	CO /nmol (TON)	HCOOH /nmol (TON)	H_2 /nmol (TON)	F.Y.[c] /%	CO_2 red Selectivity/%
SnTPyP/SnO_2	330 (47.3)	n.d.	72.7	86 (3.5)	310 (12.4)	48 (1.9)	95.4	90.6
AlTPyP/SnO_2	130 (26.9)	n.d.	26.6	32.6 (1.3)	120 (4.8)	20.5 (0.8)	37.7	83.3

[a] Turnover number. [b] Faradaic efficiency of H_2O_2 formation. [c] Faradaic efficiency of overall reduction reactions.

[1] a) A. IPCC, *Contribution of working group I to the fifth assessment report of the intergovernmental panel on climate change* **2013**, *1*, 535; b) M. Z. Jacobson, *Energy Environ. Sci.* **2009**, *2*, 148–173; c) S. C. Peter, *ACS Energy Lett.* **2018**, *3*, 1557–1561.

[2] a) X. Liu, S. Inagaki, J. Gong, *Angew. Chem. Int. Ed.* **2016**, *55*, 14924–14950; b) H. Kumagai, Y. Tamaki, O. Ishitani, *Acc. Chem. Res.* **2022**, *55*, 978–990; c) S. Yoshino, T. Takayama, Y. Yamaguchi, A. Iwase, A. Kudo, *Acc. Chem. Res.* **2022**, *55*, 966–977.

[3] J. Hawecker, J.-M. Lehn, R. Ziessel, *Helv. Chim. Acta* **1986**, *69*, 1990–2012.

[4] a) H. Takeda, O. Ishitani, *Coord. Chem. Rev.* **2010**, *254*, 346–354; b) Y. Yamazaki, H. Takeda, O. Ishitani, *J. Photochem. Photobiol. C* **2015**, *25*, 106–137; c) E. Boutin, L. Merakeb, B. Ma, B. Boudy, M. Wang, J. Bonin, E. Anxolabéhère-Mallart, M. Robert, *Chem. Soc. Rev.* **2020**, *49*, 5772–5809; d) A. Wagner, C. D. Sahm, E. Reisner, *Nat. Catal.* **2020**, *3*, 775–786; e) Y. Kou, Y. Nabetani, D. Masui, T. Shimada, S. Takagi, H. Tachibana, H. Inoue, *J. Am. Chem. Soc.* **2014**, *136*, 6021–6030; f) Y. Kou, S. Nakatani, G. Sunagawa, Y. Tachikawa, D. Masui, T. Shimada, S. Takagi, D. A. Tryk, Y. Nabetani, H. Tachibana, H. Inoue, *J. Catal.* **2014**, *310*, 57–66; g) Y. Kou, Y. Nabetani, R. Nakazato, N. V. Pratheesh, T. Sato, S. Nozawa, S.-i. Adachi, H. Tachibana, H. Inoue, *J. Catal.* **2022**, *405*, 508–519.

[5] a) J.-M. Lehn, R. Ziessel, *J. Organomet. Chem.* **1990**, *382*, 157–173; b) Y. Tamaki, T. Morimoto, K. Koike, O. Ishitani, *Proc. Natl. Acad. Sci. USA* **2012**, *109*, 15673–15678; c) C. M. Boudreaux, N. P. Liyanage, H. Shirley, S. Siek, D. L. Gerlach, F. Qu, J. H. Delcamp, E. T. Papish, *Chem. Commun.* **2017**, *53*, 11217–11220.

[6] a) S. Sato, T. Morikawa, T. Kajino, O. Ishitani, *Angew. Chem. Int. Ed.* **2013**, *52*, 988–992; b) K. Kamada, J. Jung, T. Wakabayashi, K. Sekizawa, S. Sato, T. Morikawa, S. Fukuzumi, S. Saito, *J. Am. Chem. Soc.* **2020**, *142*, 10261–10266; c) P. Kang, C. Cheng, Z. Chen, C. K. Schauer, T. J. Meyer, M. Brookhart, *J. Am. Chem. Soc.* **2012**, *134*, 5500–5503; d) W.-H. Wang, Y. Himeda, J. T. Muckerman, G. F. Manbeck, E. Fujita, *Chem. Rev.* **2015**, *115*, 12936–12973; e) R. O. Reithmeier, S. Meister, B. Rieger, A. Siebel, M. Tschurl, U. Heiz, E. Herdtweck, *Dalton Trans.* **2014**, *43*, 13259–13269.

[7] a) K. Kim, P. Wagner, K. Wagner, A. J. Mozer, *Energy Fuels* **2022**, *36*, 4653–4676; b) H. Takeda, K. Ohashi, A. Sekine, O. Ishitani, *J. Am. Chem. Soc.* **2016**, *138*, 4354–4357; c) H. Takeda, H. Kamiyama, K. Okamoto, M. Irimajiri, T. Mizutani, K. Koike, A. Sekine, O. Ishitani, *J. Am. Chem. Soc.* **2018**, *140*, 17241–17254.

[8] a) H. H. Cramer, B. Chatterjee, T. Weyhermüller, C. Werlé, W. Leitner, *Angew. Chem. Int. Ed.* **2020**, *59*, 15674–15681; b) T. Shimoda, T. Morishima, K. Kodama, T. Hirose, D. E. Polyansky, G. F. Manbeck, J. T. Muckerman, E. Fujita, *Inorg. Chem.* **2018**, *57*, 5486–5498; c) T. Ouyang, H.-H. Huang, J.-W. Wang, D.-C. Zhong, T.-B. Lu, *Angew. Chem. Int. Ed.* **2017**, *56*, 738–743.

[9] a) J. Du, B. Cheng, H. Yuan, Y. Tao, Y. Chen, M. Ming, Z. Han, R. Eisenberg, *Angew. Chem. Int. Ed.* **2023**, *62*, e202211804; b) D. Hong, Y. Tsukakoshi, H. Kotani, T. Ishizuka, T. Kojima, *J. Am. Chem. Soc.* **2017**, *139*, 6538–6541; c) D. Hong, T. Kawanishi, Y. Tsukakoshi, H. Kotani, T. Ishizuka, T. Kojima, *J. Am. Chem. Soc.* **2019**, *141*, 20309–20317.

[10] a) H. Takeda, C. Cometto, O. Ishitani, M. Robert, *ACS Catal.* **2017**, *7*, 70–88; b) D. C. Fabry, H. Koizumi, D. Ghosh, Y. Yamazaki, H. Takeda, Y. Tamaki, O. Ishitani, *Organometallics* **2020**, *39*, 1511–1518; c) M. Bourrez, M. Orio, F. Molton, H. Vezin, C. Duboc, A. Deronzier, S. Chardon-Noblat, *Angew. Chem. Int. Ed.* **2014**, *53*, 240–243.

[11] a) G. F. Manbeck, E. Fujita, *J. Porphyrins Phthalocyanines* **2015**, *19*, 45–64; b) J. Bonin, A. Maurin, M. Robert, *Coord. Chem. Rev.* **2017**, *334*, 184–198; c) L. Chen, G. Chen, C.-F. Leung, C. Cometto, M. Robert, T.-C. Lau, *Chem. Soc. Rev.* **2020**, *49*, 7271–7283.

[12] D. Saito, Y. Tamaki, O. Ishitani, *ACS Catal.* **2023**, *13*, 4376–4383.

[13] a) Y. Tamaki, K. Koike, O. Ishitani, *Chem. Sci.* **2015**, *6*, 7213–7221; b) Y. Tamaki, O. Ishitani, *ACS Catal.* **2017**, *7*, 3394–3409; c) Y. Tamaki, T. Morimoto, K. Koike, O. Ishitani, *Proc. Natl. Acad. Sci. USA* **2012**, *109*, 15673–15678.

[14] a) G. Sahara, H. Kumagai, K. Maeda, N. Kaeffer, V. Artero, M. Higashi, R. Abe, O. Ishitani, *J. Am. Chem. Soc.* **2016**, *138*, 14152–14158; b) H. Kumagai, G. Sahara, K. Maeda, M. Higashi, R. Abe, O. Ishitani, *Chem. Sci.* **2017**, *8*, 4242–4249; c) R. Kamata, H. Kumagai, Y. Yamazaki, M. Higashi, R. Abe, O. Ishitani, *J. Mater. Chem. A* **2021**, *9*, 1517–1529.

[15] a) S. Yoshino, A. Iwase, Y. Yamaguchi, T. M. Suzuki, T. Morikawa, A. Kudo, *J. Am. Chem. Soc.* **2022**, *144*, 2323–2332; b) A. Iwase, S. Yoshino, T. Takayama, Y. H. Ng, R. Amal, A. Kudo, *J. Am. Chem. Soc.* **2016**, *138*, 10260–10264; c) K. Iizuka, T. Wato, Y. Miseki, K. Saito, A. Kudo, *J. Am. Chem. Soc.* **2011**, *133*, 20863–20868.

[16] a) W.-H. Cheng, M. H. Richter, I. Sullivan, D. M. Larson, C. Xiang, B. S. Brunschwig, H. A. Atwater, *ACS Energy Lett.* **2020**, *5*, 470–476; b) S. Sato, T. Arai, T. Morikawa, *Nanotechnology* **2018**, *29*, 034001; c) H. Zhang, J. Ming, J. Zhao, Q. Gu, C. Xu, Z. Ding, R. Yuan, Z. Zhang, H. Lin, X. Wang, J. Long, *Angew. Chem. Int. Ed.* **2019**, *58*, 7718–7722; d) J. Zhao, L. Huang, L. Xue, Z. Niu, Z. Zhang, Z. Ding, R. Yuan, X. Lu, J. Long, *J. Energy Chem.* **2023**, *79*, 601–610.

[17] a) H. Inoue, T. Shimada, Y. Kou, Y. Nabetani, D. Masui, S. Takagi, H. Tachibana, *ChemSusChem* **2011**, *4*, 173–179; b) F. Kuttassery, S. Mathew, D. Yamamoto, S. Onuki, Y. Nabetani, H. Tachibana, H. Inoue, *Electrochemistry* **2014**, *82*, 475–485; c) F. Kuttassery, S. Mathew, S. N. Remello, A. Thomas, K. Sano, Y. Ohsaki, Y. Nabetani, H. Tachibana, H. Inoue, *Coord. Chem. Rev.* **2018**, *377*, 64–72.

[18] a) T. Soltani, A. Yamamoto, S. P. Singh, A. Anzai, E. Fudo, A. Tanaka, H. Kominami, H. Yoshida, *ACS Appl. Energ. Mater.* **2021**, *4*, 6500–6510; b) L.-W. Wei, S.-H. Liu, H. P. Wang, *ACS Appl. Mater. Interfaces* **2023**, *15*, 25473–25483.

[19] F. Kuttassery, H. Kumagai, R. Kamata, Y. Ebato, M. Higashi, H. Suzuki, R. Abe, O. Ishitani, *Chem. Sci.* **2021**, *12*, 13216–13232.

[20] a) A. Thomas, F. Kuttassery, S. Mathew, S. N. Remello, Y. Ohsaki, D. Yamamoto, Y. Nabetani, H. Tachibana, H. Inoue, *J. Photochem. Photobiol. A* **2018**, *358*, 402–410; b) S. Mathew, A. Sebastian, F. Kuttassery, S. Takagi, H. Tachibana, H. Inoue, *Inorg. Chim. Acta* **2021**, *526*, 120529; c) A. Thomas, Y. Ohsaki, R. Nakazato, F. Kuttassery, S. Mathew, S. N. Remello, H. Tachibana, H. Inoue, *Molecules* **2023**, *28*, 1882.

[21] F. Kuttassery, S. Mathew, H. Tachibana, H. Inoue, *Sustain. Energy Fuels* **2020**, *4*, 1945–1953.

[22] a) E. Sundin, M. Abrahamsson, *Chem. Commun.* **2018**, *54*, 5289–5298; b) M. A. Othman, B. H. Ahmad, N. F. Amat, *J. Semicond. Tech. Sci.* **2013**, *13*, 635–646.

[23] a) F. Kuttassery, S. Mathew, S. Sagawa, S. N. Remello, A. Thomas, D. Yamamoto, S. Onuki, Y. Nabetani, H. Tachibana, H. Inoue, *ChemSusChem* **2017**, *10*, 1909–1915; b) Y. Ohsaki, A. Thomas, F. Kuttassery, S. Mathew, S. N. Remello, T. Shimada, T. Ishida, S. Takagi, H. Tachibana, H. Inoue, *J. Photochem. Photobiol. A* **2020**, *401*, 112732.

[24] G. Boschloo, A. Hagfeldt, *J. Phys. Chem. B* **2001**, *105*, 3039–3044.

[25] a) K. Takamura, C. Matsubara, *Bull. Chem. Soc. Jpn.* **2003**, *76*, 1873–1888; b) F. Kuttassery, A. Sebastian, S. Mathew, H. Tachibana, H. Inoue, *ChemSusChem* **2019**, *12*, 1939–1948.
[26] F. Kuttassery, S. Sagawa, S. Mathew, Y. Nabetani, A. Iwase, A. Kudo, H. Tachibana, H. Inoue, *ACS Appl. Energ. Mater.* **2019**, *2*, 8045–8051.
[27] a) K. Fuku, K. Sayama, *Chem. Commun.* **2016**, *52*, 5406–5409; b) S. G. Patra, A. Mizrahi, D. Meyerstein, *Acc. Chem. Res.* **2020**, *53*, 2189–2200; c) T. M. Gill, L. Vallez, X. Zheng, *ACS Energy Lett.* **2021**, *6*, 2854–2862; d) L. Fan, X. Bai, C. Xia, X. Zhang, X. Zhao, Y. Xia, Z.-Y. Wu, Y. Lu, Y. Liu, H. Wang, *Nat. Commun.* **2022**, *13*, 2668; e) L. Li, Z. Hu, Y. Kang, S. Cao, L. Xu, L. Yu, L. Zhang, J. C. Yu, *Nat. Commun.* **2023**, *14*, 1890.

Manuscript received: June 26, 2023
Accepted manuscript online: July 26, 2023
Version of record online: August 24, 2023